Journal of Engineering Science 15(2), 2024, 41-50
DOI: https://doi.org/10.3329/jes.v15i2.82161

JES
an international Journal

INVESTIGATION OF THE VERTICAL STRUCTURE OF TROPICAL CYCLONES BY WRF MODEL

Kh. Hafizur Rahman[1, 2*], M. A. Taher[2]

[1] *Bangladesh Meteorology Department, Agargaon, Dhaka.*

[2] *Department of Mathematics, Dhaka University of Engineering & Technology, Gazipur-1700*

Received: 15 October 2024 Accepted: 24 November 2024

ABSTRACT

Tropical cyclones (TCs) are the most destructive atmospheric phenomena regarding damage to lives and properties over the coastal regions. An attempt has been made to examine the vertical structure of two TCs (Amphan and Bulbul) formed over the Bay of Bengal (BoB) with unlike intensities. Weather Research and Forecasting (WRF) model is deployed to simulate the selected TCs. The model is configured with two two-way interactive nested domains with a horizontal resolution of 27 km and 9 km. Outputs from the 9 km domain are considered for analysis. The vertical structure of different parameters like tangential and radial wind, relative humidity, vorticity, vertical velocity, etc. are examined. WRF model is capable enough to simulate the vertical structure of different parameters. It was found that Amphan's structure is simulated realistically better as compared to Bulbul. Investigation of the vertical structure of TCs would enhance the knowledge in understanding the role of vertical structure in predicting TCs intensity as well as movement.

Keywords: *Bay of Bengal, Tropical Cyclone, Vertical Structure, WRF*

1. INTRODUCTION

The Indian subcontinent is one of the most horrible affected regions due to tropical cyclones in the biosphere. The subcontinent with an extended coastline is experienced to nearly 7-10% (Mondal et al., 2021) of the global tropical cyclones. Most of the tropical cyclones have their initial genesis over the Bay of Bengal (BoB) and strike the east coast of India and Bangladesh coast. Typically, five to six tropical cyclones form each year, out of these two or three can be attained severity. The number of cyclones that occur in the BoB is higher than the Arabian Sea and the ratio is about 4:1 (Dube et al., 1977). This is probably because the Sea Surface Temperature (SST) over the Arabian Sea is cooler than that of over the BoB. Furthermore, the passage of west-moving remnants of the TCs forming in the West Pacific Ocean over the BoB also helps in additional cyclogenesis over the BoB.

TCs are the greatest destructive natural catastrophes with huge potential for damage to lives and properties. The damage is mainly due to heavy rainfall, strong winds, and accompanying storm surges (Mohapatra et al., 2015). Every year the people of tropical regions encounter these natural calamities. It is a warm core vortex where the wind blows anti-clockwise in the northern hemisphere and clockwise in the southern hemisphere. When wind speed exceeds 17 m/s it is termed as tropical cyclone in the Indian Ocean. TCs are also denoted as 'Hurricanes' over the Atlantic Ocean, 'Typhoons' over the Pacific Ocean, and 'Willy-Willy' over the Australian Seas. The strength of a TC is measured by the horizontal wind speed at a 10-meter height and the central pressure drop. Wind speeds that measure the strength of TCs are the tangential components of horizontal wind which is known as primary circulation. TCs may differ significantly from one to another, and from day to day, in intensity, size, structure, spiral banding, eye feature, and degree of symmetry (Kepert, 2010). The size of the storm can be as wide as 300 km and the eye can be as wide as 50 km (Emanuel, 2005).

Accurate and timely forecasting of TC path, intensity, and landfall area is very critical for disaster management. The precision of track forecasts has advanced significantly over the past decades owing to progress in Numerical Weather Prediction (NWP) models (Heming and Goerss, 2010). However, still substantial errors in track forecast, more than 1,000 km beyond 72 hours exist and break further improvement of the yearly mean error (Yamaguchi et al., 2012). The radial organization of the primary rotation was extensively studied in past years (Mallen et al., 2005), and the vertical organization received comparatively less consideration over the BoB region. This is a probable lack of quality observations of wind data. Nevertheless, it is very significant to understand the vertical structure of TC. The inner core of a TC is subjugated by robust convective activity and overwhelming winds and the outer area is dominated by lashing rain accompanied by severe storm surges and floods. The vertical structure is crucial in understanding the various processes that cause precipitation as well as strong winds. Henceforth, a comprehensive study of the vertical structure of the TC is vital.

*Corresponding Author: rs77_hafizbmd@yahoo.com

ISSN 2075-4914 (print); ISSN 2706-6835 (online)

Several studies on the vertical structure of TCs were conducted based on observations of other oceanic basins. The vertical structure of radial and tangential winds for two TCs over the southwest Pacific region was conducted by compositing observation data (Holland and Merrill, 1984). The upper-level outflow near 200 mb, the secondary influx region near 400 mb, and the low-level influx examined. The low-level influx supplies an import of angular motion to balance the frictional dissipation and strengthen the TC. A composite study was conducted using the northwest Pacific upper air data to analyze the vertical structure of TCs (Frank, 1977). Various fields such as temperature, height, humidity, wind, and vertical velocity were analyzed. Another study based on observations was conducted over the North Atlantic basin to investigate the vertical organization of tangential wind (Stern and Nolan, 2009). The results showed that the outer slope of the Radius of Maximum Wind (RMW) with elevation is not correlated with the TC intensity. Vertical wind profiles of hurricanes were studied using GPS sondes and Doppler radar data (Giammanco et al., 2012). The result indicates that inside the boundary layer, wind profiles displayed a logarithmic rise with altitude up to the height of maximum wind. The organization of rainbands in the TC was studied using TRMM precipitation radar (Hence and Houze, 2012). The results show two layers of structures of the rainbands are separated by the melting layer. The rainbands located more than 200 km from the eye revealed greater convective activity compared to the inner rainbands. The aircraft exploration data were used to determine the correlation between TC height and intensity (DesRosiers, 2023). The result shows that the vertical extension of the TC wind field is highly correlated with the current intensity of the TC. Recently, the brightness temperature data were used to identify the vertical orientation of the TC over the NIO (Uma and Reshma, 2024). They found a broader dispersal of reflectivity and vertically stretched compared to that of other basins.

The Weather Research and Forecasting (WRF) model has been extensively utilized to simulate various hazardous weather phenomena, e.g. heavy rainfall, tropical cyclones, etc, and real-time NWP globally (Routray et al., 2010; Osuri et al., 2012). National Hydrological and Meteorological Centers of different nations are making predictions of TCs operationally. In the present study, two TCs ‘Amphan’ and ‘Bulbul’ of dissimilar intensities are selected to study vertical structure with the support of the Advanced Research version of the WRF model.

2. BRIEF DESCRIPTION OF THE SYSTEMS

2.1 Amphan

The Super Cyclonic Storm ‘Amphan’ was initiated over Southeast BoB and adjacent to the South Andaman Sea on 13 May 2020 morning. It was concentrated into a well-marked low on 14 May 2020 morning, then into a depression over the Southeast BoB on 16 May 2020 in the early morning. The system further deepened into a deep depression on 16 May 2020 in the afternoon, moved north-northwestwards, and intensified into Cyclonic Storm ‘Amphan’ over the Southeast BoB on 16 May 2020 in the evening. It was moved closely northwards and further deepened into a Severe Cyclonic Storm over the Southeast BoB on 17 May 2020 in the morning. The system experienced rapid strengthening during the following day and consequently deepened into a Very Severe Cyclonic Storm (VSCS) on 17 May 2020 afternoon, an Extremely Severe Cyclonic Storm (ESCS) on 18 May 2020 early hours, and into a Super Cyclonic Storm on 18 May 2020 noon. The system sustained its intensity of a Super Cyclonic Storm over the West-central BoB for about 24 hours. Subsequently, it weakened and crossed the West Bengal-Bangladesh coasts as a VSCS, near latitude 21.65°N and longitude 88.3°E by the evening of 20 May 2020, with a maximum wind speed of 185 km/h (Report by RSMC, New Delhi, 2020). The observed track of ‘Amphan’ is presented in Figure 1(a).

2.2 Bulbul

The Very Severe Cyclonic Storm (VSCS) ‘Bulbul’ was initiated from the remnant of severe tropical storm ‘Matmo’ over the West Pacific Ocean that emerged into the North Andaman Sea. It originated as a low over the North Andaman Sea on 04 November 2019 in the early morning. Concentrating into a well-marked low over the North Andaman Sea and adjacent area, the system was moved west-northwestwards and further intensified into a Depression over east central and adjacent southeast BoB on 05 November 2019 early morning and into a deep depression (DD) over the same area on 06 November 2019 early morning. The system was moved north-northwestwards and deepened into a TC ‘Bulbul’ at late night on 06 November 2019 over Eastcentral and adjacent southeast BoB. Continuous moving north-northwestwards the system intensified into a severe cyclonic storm (SCS) on 07 November 2019 evening over West-central and adjoining East-central BoB. Further moving northwards, the SCS ‘Bulbul’ intensified into a VSCS on the early morning of 08 November 2019 over the west-central and adjoining east-central BoB. The system was moved nearly northwards till the afternoon of 09 November 2019 and then re-curved northeastwards onward the evening of 09 November 2019. Sequentially, the system was weakened into a SCS and crossed the West Bengal coast near the latitude 21.55°N and longitude 88.5°E by midnight of 09 November 2019 as a SCS with a maximum wind speed of 135 km/h. It then moved

northeastwards and weakened into a cyclonic storm over coastal Bangladesh and adjacent areas in the early morning of 10 November (Report by RSMC, New Delhi, 2019). The observed track of 'Bulbul' is presented in Figure 1(b).

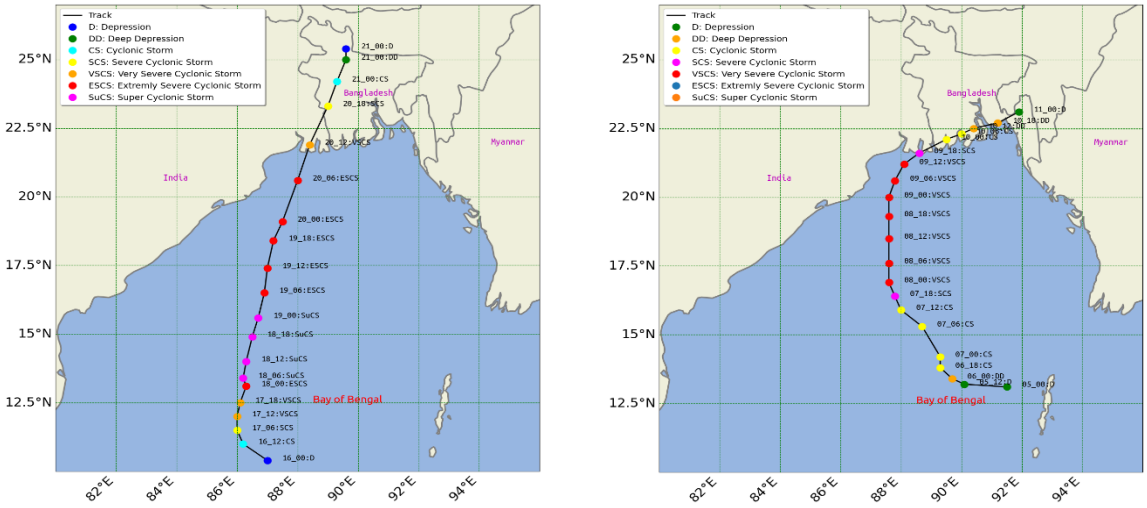

Figure 1. Observed track of Cyclone (a) Amphan and (b) Bulbul. Markers with different colors represent various intensity stages.

3. EXPERIMENTAL DESIGN

The non-hydrostatic, compressible WRF model was developed by the National Center for Atmospheric Research (NCAR). Key features include a fully compressible, Eulerian non-hydrostatic equation set, a terrain-following vertical coordinate system based on hydrostatic pressure, and a constant-pressure surface at the model's top level. The model employs a staggered grid, similar to the Arakawa-C grid, and utilizes a third-order Runge-Kutta time integration scheme for horizontal and vertical calculations. The WRF model integrates multiple physical processes, such as microphysics (MP), cumulus parameterization (CP), planetary boundary layer (PBL), surface layer, land surface interactions, and both longwave and shortwave radiation, each with multiple configurable options (Shamrock et al., 2019). Model input details are presented in Table 1, and the selected model domain for the study is shown in Figure 2. The model initialization was accepted with lead times of 120, 96, 72, 48, and 24 hours before landfall to assess performance at varying forecast lead times.

Table 1. Brief description of WRF model configuration

Model	WRF V4.2
Max_domain	2
Map Projection	Mercator
Resolution	27 km, 9 km
Time step	108s,36s
Central point of the domain	17.5^0 N, 87.5^0E
No. Of grid points	152, 265(WE); 144, 298(NS)
No. Of Vertical levels	42 Sigma Levels
Horizontal Grid	Arakawa C Grid
Time Integration	Runge-Kutta second and third-order time
Radiation Scheme	Dudhia's short-wave/RRTM long-wave
PBL Scheme	YSU scheme
Convection	Kain-Fritsch (new Eta) scheme
Micro Physics	WSM3-class simple ice scheme

4. DATA USED

The initial and boundary conditions for the WRF model are derived from the Global Tropospheric Analyses and Forecast Grids data (at a 0.25°×0.25° resolution) provided by the Global Data Assimilation System (GDAS)/Final Analyses (FNL) from the National Centers for Environmental Prediction (NCEP). While the Sea Surface Temperature (SST) remains constant throughout the model integration, the lateral boundary conditions are refreshed every 6 hours. The United States Geological Survey (USGS) terrain data, at a 10-minute resolution, was

incorporated into the WRF preprocessing system to represent topography accurately. Model performance, particularly in predicting tropical cyclone tracks and intensity, was validated using RSMC New Delhi's best track data sets (tracks are not shown in the figure), utilizing various initial conditions to identify the optimal one for analyzing vertical structure.

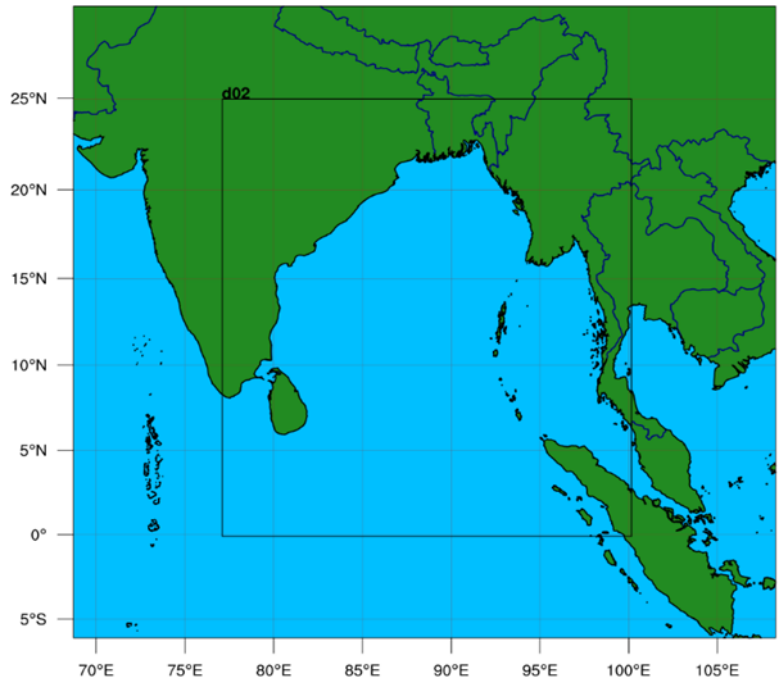

Figure 2. Model domain selected for the study. The outer domain grid size is 27 km and the inner domain grid size is 9 km.

5. RESULTS AND DISCUSSION

The vertical structure of various parameters is investigated at peak intensity simulated by the model for the selected TCs. Amphan peak intensity was found at 18 UTC on 18 May 2020 based on the 00 UTC 18 on May 2020 initial condition, on the other hand, Bulbul peak intensity was found at 15 UTC on 07 Nov 2019 based on 00 UTC on 06 Nov 2019 initial condition. Simulated maximum surface wind speed is found 111 kts and 70 kts for Amphan and Bulbul respectively. The model underestimates the intensity of the TCs by 19 kts and 5 kts for Amphan and Bulbul respectively. Longitudinal height cross section is accomplished through the center position i.e., latitude 15.54^0 N & longitude 86.4^0 E and latitude 16.14^0 N & longitude 88.15^0 E for Amphan and Bulbul respectively. The center of the TC is fixed by calculating Minimum Sea Level Pressure (MSLP). As there are no observational facilities for the vertical structure of TCs over the BoB region available, the results of the study are compared with the previous studies over other oceanic basins based on observation data. Tangential, radial, and vertical wind structures were reasonably well captured by the model as compared to TC structure over other basins based on observation data (Frank, 1977; Holland and Merrill, 1984; Stern and Nolan, 2009). The vertical structure of other parameters such as relative humidity, relative vorticity, and water vapor mixing ratio is also reasonably simulated by the model as compared to previous studies based on observations as well as reanalysis data over other basins (Frank, 1977; Huang and Zheng, 2020). The model predicted vertical extension of the wind field for Amphan and Bulbul suggested that vertical extension of the wind field is highly correlated to TC intensity which is justified by recent studies (DesRosiers et al., 2023).

5.1 Tangential Wind

The tangential wind is a vital parameter of TCs. TC intensity is measured by the strength of the tangential wind speed. The model simulated vertical cross-section of tangential wind is presented in Figure 3. At 18 UTC on 18 May 2020, the center of Amphan was located near latitude 15.54^0 N & longitude 86.4^0 E, clearly depicting the widest cyclonic flow in the lower level of the atmosphere, which is reduced in horizontal extent along the vertical direction. At about 800 hPa, gale wind (20 m/s) is extended horizontally up to 500 km from the center which is reduced to 180 km at 300 hPa, and at 200 hPa it is limited to about 70 km for Amphan as shown in figure 3(a). Again, at 15 UTC on 07 Nov 2019, the center of Bulbul is located near latitude 16.14^0 N & longitude 88.15^0 E presented in Figure 3(b), it is seen that near 800 hPa, 20 m/s wind is horizontally extended up to 200 km from the

center and at 400 hPa it is reduced to 70 km for Bulbul. There is anticyclonic circulation above the cyclonic flow at different levels indicated by zero contour line for both the systems. The speed of tangential wind is found maximum at the top of the planetary boundary layer close to 900hPa. Tangential wind speed almost linearly decreases with increasing height and becomes zero. Gale wind (20 ms^{-1}) is extended up to 200 hPa for Amphan and Bulbul it is extended just up to 400 hPa level. This is due to the variation in intensity of the two cyclones.

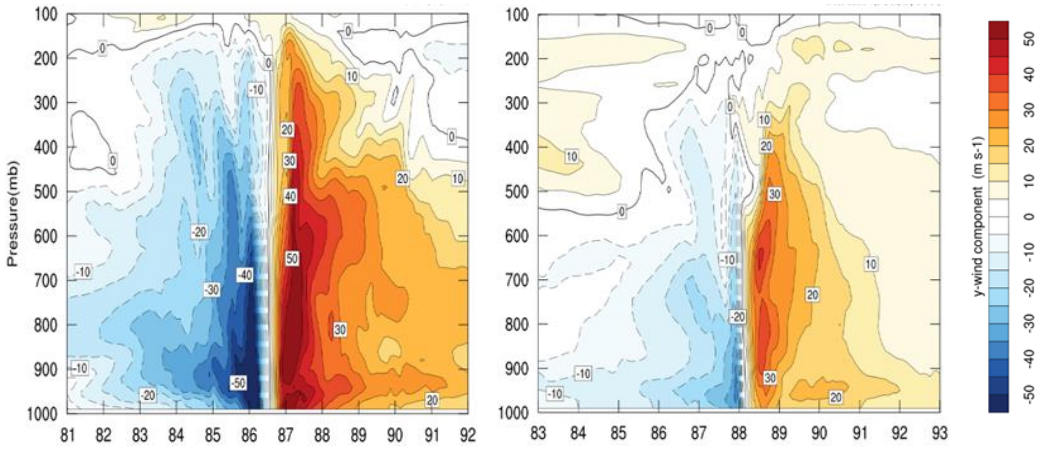

(a) (b)

Figure 3. Longitudinal height cross section of tangential wind (y-component) of (a) Amphan and (b) Bulbul.

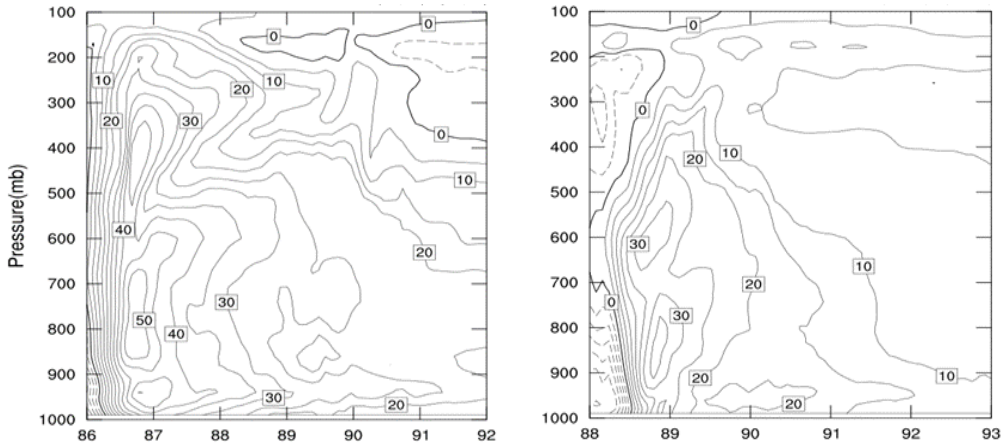

(a) (b)

Figure 4. As in Figure 3, without shade. Cross section is done from the center to east of the systems (a) Amphan and (b) Bulbul.

Again, there is no significant outward slope of the RMW just above the boundary layer for cyclone Amphan as shown in Figure 4(a). The slope of the RMW above the boundary layer shifts outward with height for Bulbul as shown in Figure 4(b). The tangential wind speed is decreased as the radius is increased for both cases. As the intensity of Amphan is higher than that of Bulbul, the outer slope of the RMW is seen for Bulbul. The results discussed are consistent with the vertical structure of Typhoons over the South China Sea (Huang and Zheng, 2020).

5.2 Radial Wind

The radial wind is the minor circulation of TCs. Radial influx is initiated by friction in the boundary layer and outflux is driven by forced uplift from below and the pressure gradient linked with upper-level anti-cyclone (Zarzycki and Jablonowski, 2015). At 18 UTC on 18 May 2020, the center of Amphan was located near latitude 15.54^0 N & longitude 86.4^0 E, and maximum inflow is found near the eye wall where the pressure gradient is maximum. Maximum inflow is found in the planetary boundary layer, below 900 hPa level with maximum value to the west of Amphan as shown in Figure 5(a). Maximum outflow is found at 200 hPa level to both sides of the storm center for Amphan. Again, at 15 UTC on 07 Nov 2019, the center of Bulbul is located near latitude 16.14^0

N & longitude 88.15^0 E and depicted that relatively weak inflow is seen in the boundary layer to both sides of the system center as shown in Figure 5(b). Maximum outflow is found at 300 hPa level to both sides of the storm center in the case of Bulbul. Both radial inflow at the lower level and upper-level outflow are considerably stronger in Amphan than in Bulbul, suggesting a much stronger circulation. In the intermediate layers (900-400) hPa there is inflow at large radii. The outflow layers control the movement of TCs.

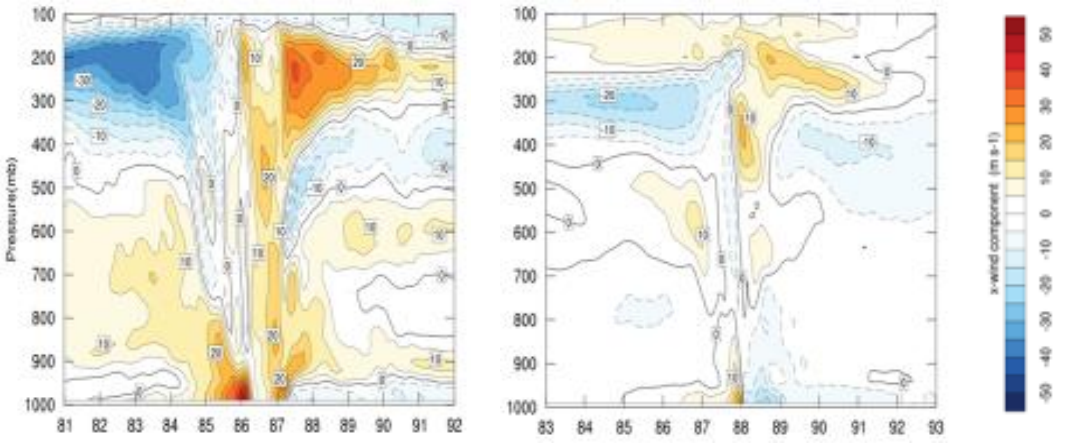

(a) (b)

Figure 5. Longitudinal height cross section of radial wind (x-component) of (a) Amphan and (b) Bulbul.

5.3 Relative Humidity

The high amount of Relative Humidity (RH) between lower and mid-levels is crucial for tropical cyclone formation and intensification. Lower moisture in the middle levels is not favorable for permitting the continuing growth of prevalent thunderstorm activity. The model simulated RH is depicted as a strong RH higher than 95% vertically extending up to 600 hPa level and 770 km horizontally across the center of Amphan as shown in Figure 6(a). At 18 UTC on 18 May 2020, the center of Amphan is located near latitude 15.54^0 N & longitude 86.4^0 E and is depicted that above 600 hPa RH decreased as height increased. The center of the storm is identified with the lower value of RH. In general, vertically, in the center, the RH decreases rapidly to about 50% at the 500 hPa level. This is due to subsidence inside the eye. There is a thin layer of dry air intrusion between 600-800 hPa levels to the west of the system which is about 300 km away from the system center. At 15 UTC on 07 Nov 2019, a vertical cross-section through the center of Bulbul near latitude 16.14^0 N & longitude 88.15^0 E depicted that a strong RH higher than 95% is only at lower levels of Bulbul as shown in Figure 6(b). Cyclone center is not identified as Amphan. There is a deep layer of dry air intrusion between 450-700 hPa levels to the west of the system which is about 100 km away from the center. Intrusion of dry air is a possible reason for hampering further intensification of Bulbul. The results are consistent with the vertical structure of RH over the South China Sea (Huang and Zheng, 2020).

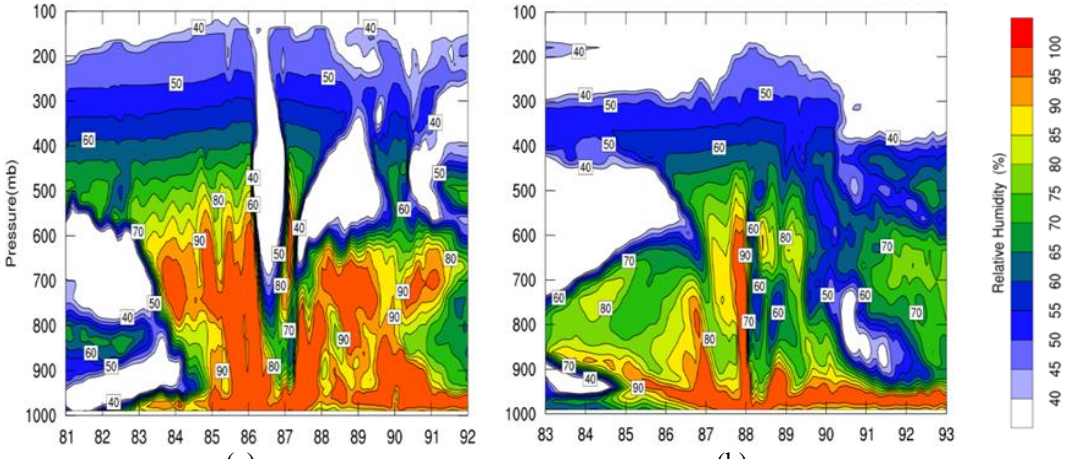

(a) (b)

Figure 6. Longitudinal height cross section of relative humidity (a) Amphan and (b) Bulbul. Relative humidity less than 40% is shaded white.

5.4 Relative Vorticity

A perpendicular cross-section of the model simulated Relative Vorticity (RV) is presented in Figure 7. Cross-section is done through the center of Amphan (15.54^0 N/86.4^0 E, as at 18 UTC on 18 May 2020) and Bulbul (16.14^0 N/ 88.15^0 E, as at 15 UTC on 07 Nov 2019). As in the figure, strong positive RV is seen at lower levels near the center with maximum values of $408\times10^{-5}s^{-1}$ and $465\times10^{-5}s^{-1}$ for Amphan and Bulbul respectively. The spatial coverage of RV for Amphan shown in Figure 7(a) is twice that of Bulbul shown in Figure 7(b). Vertical extension of RV is up to 100 hPa for Amphan and it is below 300 hPa for Bulbul. Positive RV decreases with increasing height and becomes zero and then negative for both TCs. In the case of Amphan, there is negative RV at about 300-400 hPa levels to the east of the system. There is another core of negative RV between 100-300 hPa levels just to the west of the system. In the case of Bulbul, there is negative vorticity between 300-400 hPa levels above the center. Again, contour analyses without shades show that RV center is almost coincided with the MSLP center for Amphan. Nevertheless, for Bulbul, the RV center is shifted eastward from the MSLP center.

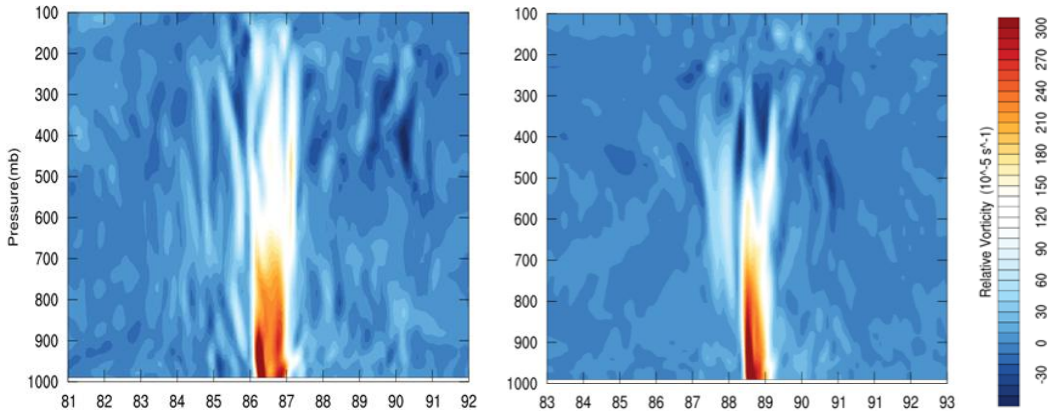

Figure 7. Longitudinal height cross section of relative vorticity of (a) Amphan and (b) Bulbul.

5.5 Vertical Velocity

The model simulated vertical velocity field at peak intensity is shown in Figure 8. A vertical cross-section of vertical velocity is done through the center of Amphan (15.54^0 N/86.4^0 E, as at 18 UTC on 18 May 2020) and Bulbul (16.14^0 N/ 88.15^0 E, as at 15 UTC on 07 Nov 2019). As shown in the figure, concerning ascending motion, descending motion is much weaker. Maximum ascending motion is found 4.4 ms^{-1} and 6.06 and descending motion is 1.7 ms^{-1} and 1.39 ms^{-1} for Amphan and Bulbul respectively. Upward motion is initiated at the surface for both TCs but strong upward motion is found at the upper level between 500 – 300 hPa levels for Amphan. At the same time weak downward motion is found between 200-400 hPa levels with the peak at about 300 hPa level shown in Figure 8(a). Again, for Bulbul, strong upward motion is found at two different levels i.e. between 600 - 700 hPa and 400 - 500 hPa levels separated by weak downward motion. Maximum downward motion is found at lower levels between 800 - 900 hPa levels. The upward motion at lower mid and upper levels for both TCs is stronger than the lower level. The increase in upward motion in the higher levels may be accredited to the release of latent heat (Zipser, 2003; Romps and Kuang, 2010).

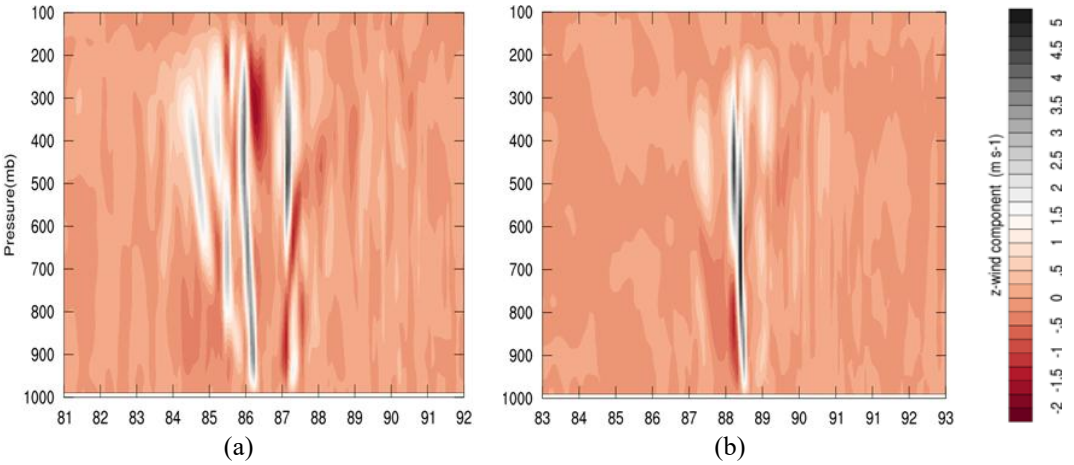

Figure 8. Longitudinal height cross-section of vertical velocity (a) Amphan and (b) Bulbul

5.6 Water Vapor Mixing Ratio

The vertical cross-section of the model simulated water vapor mixing ratio (gm/kg) is represented in Figure 9. Cross-section is done through the center of Amphan (15.54^0 N/86.4^0 E, as at 18 UTC on 18 May 2020) and Bulbul (16.14^0 N/ 88.15^0 E, as at 15 UTC on 07 Nov 2019). It is found that the main moisture source within the lower level of the atmosphere is transported upward through vertical motion. A higher value of water vapor mixing ratio is found around the center and the value is 24.9 gm/kg for Amphan as shown in Figure 9(a). Again, the maximum value of the water vapor mixing ratio is calculated 21.87 gm/kg for cyclone Bulbul as shown in Figure 9(b). Nevertheless, the higher value of the water vapor mixing ratio decreases with increasing height for both TCs. Moistures through evaporation from the ocean surface are the main energy source of TC intensification.

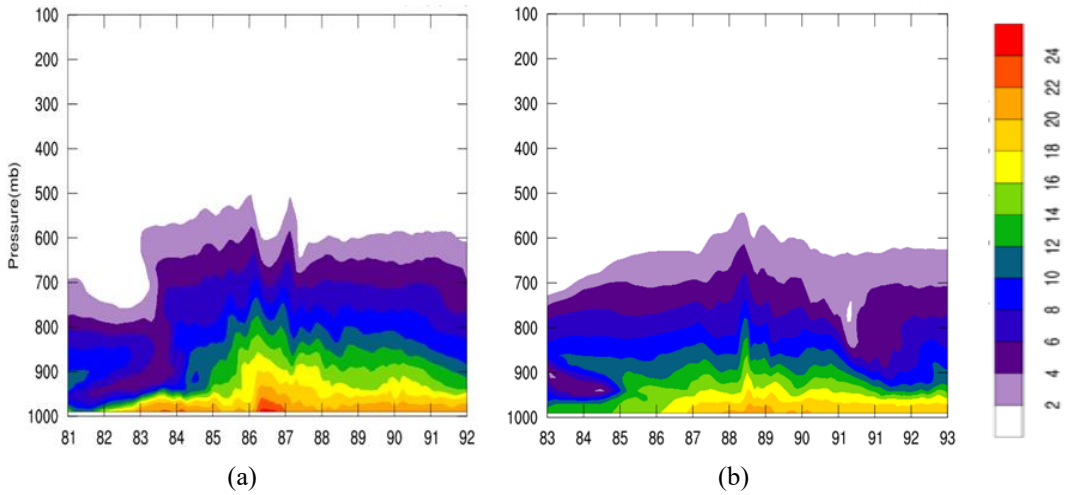

(a) (b)

Figure 9. Longitudinal height cross-section of water vapor mixing ratio (a) Amphan and (b) Bulbul

6. CONCLUSIONS

This study examined the vertical structure of dynamic and thermodynamic parameters of two TCs of different intensities. The model-derived parameters such as tangential wind, RH, RV, vertical velocity, and water vapor mixing ratio were analyzed and compared with findings from previous research.

The vertical cross-section of tangential wind exposed distinct structural differences between the two cyclones: for cyclone Amphan, the maximum wind shows minimal outward tilt with height, while for Bulbul, the wind profile tilts outward with height. The tangential wind indicates a broad cyclonic flow at lower levels that contracts with height. The radial wind revealed maximum inflow within the planetary boundary layer, below the 900 hPa level, for Amphan, while Bulbul exhibits relatively weaker inflow. The strongest outflow occurs at the 200 hPa level for Amphan and the 300 hPa level for Bulbul. The lower-level radial inflow, and the upper-level outflow, are significantly stronger in Amphan as compared to Bulbul.

The RH cross-section highlights notable features in each TC. Amphan showed minimal RH near the center whereas the center of Bulbul was not identified as Amphan. Bulbul experienced significant dry air intrusion from the west of the center between 450 and 700 hPa levels. This dry air intrusion likely contributed to Bulbul's limited intensification. The RV values were found to peak at lower levels, with maximum RVs of 408.47×10^{-5} s^{-1} for Amphan and 465.6×10^{-5} s^{-1} for Bulbul. Although Amphan was the more intense TC, its RV was lower than Bulbul. This is consistent with the expectation that in smaller TCs, wind fields are concentrated near the center, resulting in higher local vorticity, while larger TCs, despite having greater overall rotational energy, show a more distributed RV pattern (Montgomery and Smith 2014). In addition, RV extends above 200 hPa in Amphan and only to 300 hPa in Bulbul, with Amphan's RV center aligned with the MSLP center, whereas Bulbul's RV center was eastward-shifted from the MSLP center.

Regarding vertical motion, upward movement in both TCs exceeded downward motion, which was accurately represented in the model. Maximum upward motions reached 4.4 m s^{-1} in Amphan and 6.06 m s^{-1} in Bulbul, with weaker downward motions of 1.7 m s^{-1} and 1.39 m s^{-1}, respectively. This increased upward motion in the mid- and upper levels is likely due to latent heat release, as the primary moisture source at lower atmospheric levels was effectively transported upward, a process well-captured by the model. Amphan also exhibited a higher water vapor mixing ratio (24.9 g/kg) than Bulbul (21.87 g/kg). The study highlights that despite Amphan's greater intensity, Bulbul's RV and vertical velocity were higher, suggesting the need for further research to explore these

variations. Overall, this research advances our understanding of TCs' vertical structure across different parameters, enhancing capabilities for predicting TC intensity and movement.

ACKNOWLEDGMENTS

The authors are very grateful to NCEP/NCAR for providing GDAS data. Especial credit goes to WRF model developers for the study. The authors also thank their colleagues for their valuable suggestions during the study.

REFERENCES

DesRosiers, A. J., Bell, M. M., Klotzbach, P. J., Fischer, M. S., and Reasor, P. D. 2023. Observed relationships between tropical cyclone vortex height, intensity, and intensification rate. Geophysical Research Letters, 50: e2022GL101877.

Dube, S. K., Rao, A. D., Sinha, P.C., Murty, T. S., Bahulayan, N. 1977. Storm surge in the Bay of Bengal and Arabian Sea: the problem and its prediction‖. Mausam, 48:283–304.

Emanuel, K. 2005. Divine wind: the history and science of hurricanes, Chapter Genesis, 285.

Frank, W. M. 1977. The structure and energetics of the tropical cyclone, I. Storm structure. Monthly weather review, 105:1119-1135.

Giammanco, Ian M., Schroeder, John L. and Powell, Mark D. 2012. Observed characteristics of tropical cyclone vertical wind profiles. Wind and Structures, 15(1):65-86.

Heming, J. and Goerss, J. 2010. Track and structure forecasts of tropical cyclones. Global Perspectives on Tropical Cyclones. World Sci., Singapore, 133−148.

Hence, D. A. and Houze, R. A. 2012.Vertical structure of tropical cyclones with concentric eyewalls as seen by the TRMM precipitation radar. J. Atmos. Sci., 69(3):1021-1036.

Holland, G. J. and Merrill, R.T. 1984. On the dynamics of tropical cyclone Structural-changes, Q. J. Roy. Meteor. Soc., 110:723-745.

Huang, Y., and Zheng, B. 2020. Tropical cyclone structure in the South China Sea based on high-resolution reanalysis data and comparison with that of 'bogus' vortices. Dynamics of Atmospheres and Oceans, 89:101128.

Kepert, J. D. 2010. Global perspectives on tropical cyclones: From Science to Mitigation, Chapter 1 - Tropical cyclone structure and dynamics, 3–53.

Mallen, K. J., Montgomery, M. T. and Wang, B. 2005. Reexamining the near-core radial structure of the tropical cyclone primary circulation: Implications for vortex resiliency. J. Atmos. Sci., 62:408-425.

Mohapatra, M., Nayak, D.P., Sharma, M., Sharma, R.P. and Bandyopadhyay, B.K. 2015. Evaluation of official tropical cyclone landfall forecast issued by India Meteorological Department. J. Earth Syst. Sci, 124:861–874.

Mondal, M., Haldar, S., Biswas, A., Mandal, S., Bhattacharya, S. and Paul, S. 2021. Modeling cyclone-induced multi-hazard risk assessment using analytical hierarchical processing and GIS for coastal West Bengal, India. Reg Stud Mar Sci, 44:101779.

Montgomery, M. T., and Smith, R. K. 2014. Paradigms for Tropical Cyclone Intensification. Australian Meteorological and Oceanographic Journal, 64:37-66.

Osuri, K.K, Mohanty, U.C, Routray, A, Kulkarni, M.A. and Mohapatra, M. 2012. Customization of WRF-ARW Model with physical parametrization schemes for the simulation of Tropical Cyclones over the North Indian Ocean. Natural Hazards, 63:1337–1359.

Romps, D. M., and Kuang, Z. 2010. Do undiluted convective plumes exist in the upper tropical troposphere? J. Atmos. Sci., 67:468–484.

Routray, A, Mohanty, U.C, Rizvi, S.R.H, Niyogi, D., Osuri, K.K. and Pradhan, D. 2010. Impact of Doppler weather radar data on simulation of Indian monsoon depressions. Q. J. Roy. Meteor. Soc., 136:1836–1850.

RSMC, 2019. Very Severe Cyclonic Storm "BUL BUL" over the Bay of Bengal (05-11 November 2019): A Report by RSMC, New Delhi.

Shamrock, W. C., Klemp, J. B., Dudhia, J., Gill, D. O., Liu, Z., Berner, J., Wang, W., Powers, J. G., Duda, M. G., Barkar, D., & Huang, X. Y. 2019. A description of the advanced research WRF model version 4. National Center for Atmospheric Research: Boulder, CO, USA, 145.

Stern, D. P. and Nolan, D. S. 2009. Reexamining the vertical structure of tangential winds in tropical cyclones: Observation and theory. J. Atmos. Sci., 66:3579- 3600.

Super Cyclonic Storm "AMPHAN‟ over Southeast Bay of Bengal (16-21 May 2020): A Report by RSMC, New Delhi, India.

Uma, K.N., and Reshma, B. 2024. Vertical structure of North Indian Ocean tropical cyclones: A composite analysis using TRMM and GPM. Dynamics of Atmospheres and Oceans, 105:101421.

Yamaguchi, M., Nakazawa, T. and Aonashi, K. 2012. Tropical cyclone track forecasts using JMA model with ECMWF and JMA initial conditions. Geophys. Res. Lett., 39: L09801.

Zarzycki, Colin & Jablonowski, Christiane. 2015. Experimental Tropical Cyclone Forecasts Using a Variable-Resolution Global Model. Monthly Weather Review, 143(10):4012-4037.

Zipser, E. J. 2003. Some views on ‘‘hot towers’’ after 50 years of tropical field programs and two years of TRMM data. Cloud Systems, Hurricanes, and the Tropical Rainfall Measuring Mission (TRMM), Meteor. Monogr. No. 51, Amer. Meteor. Soc., 49–58.